Atmos. Chem. Phys. Discuss., https://doi.org/10.5194/acp-2018-1041
Manuscript under review for journal Atmos. Chem. Phys.
Discussion started: 20 November 2018

Atmospheric Chemistry and Physics Discussions

Atmospheric measurements of the terrestrial O_2 :CO_2 exchange ratio of a mid-latitude forest

Mark O. Battle[1], J. William Munger[2], Margaret Conley[1], Eric Sofen[1], Rebecca Perry[1], Ryan Hart[1], Zane Davis[1], Jacob Scheckman[1], Jayme Woogerd[1], Karina Graeter[1], Samuel Seekins[1], Sasha David[1], and John Carpenter[1]

[1]Dept. of Physics & Astronomy, Bowdoin College, Brunswick ME 04011-8488 USA
[2]School of Engineering and Applied Sciences, Harvard University, Cambridge, MA 02138 USA

Correspondence: Mark O. Battle (mbattle@bowdoin.edu)

Abstract.

Measurements of atmospheric O_2 have been used to quantify large-scale fluxes of carbon between the oceans, atmosphere and land since 1992 (Keeling and Shertz, 1992). With time, datasets have grown and estimates of fluxes have become more precise, but a key uncertainty in these calculations is the exchange ratio of O_2 and CO_2 associated with terrestrial photosynthesis and respiration (α_B). We present measurements of atmospheric O_2 and CO_2 collected over a six-year period from a mixed deciduous forest in central Massachusetts, USA (42.537°N, 72.171°W). Using a differential fuel-cell based instrument for O_2 and a non-dispersive infrared analyzer for CO_2, we analyzed an airstream collected within and $\sim$ 6m above the forest canopy. Averaged over the entire period of record, we find these two species covary with a slope of -1.058 ± 0.006 moles of O_2 per mole of CO_2. If we limit the data to values collected on summer days within the canopy, the slope is -1.01 ± 0.01. These are the conditions in which biotic influences are most likely to dominate, suggesting that this slope is our best estimate of α_B. This result is significantly different from value of 1.1 widely used in O_2-based calculations of the global carbon budget, suggesting adjustments of these O_2-based flux estimates may be in order.

atmospheric O_2/N_2, oxidative ratio, terrestrial carbon sink

1 Introduction

Since the pioneering work of Keeling and Shertz (1992), measurements of the abundance of atmospheric O_2 and CO_2 have been used extensively for constraining fluxes of carbon to and from the land biosphere and the oceans. In a conceptual form, the simplest budgets for atmospheric O_2 and CO_2 can be written

$$\frac{dO_2}{dt} = \alpha_{ff}\ f_{ff}\ + \alpha_B\ f_{land}$$

$$\frac{dCO_2}{dt} = f_{ff}\ + f_{land}\ + f_{ocean}$$

Atmos. Chem. Phys. Discuss., https://doi.org/10.5194/acp-2018-1041
Manuscript under review for journal Atmos. Chem. Phys.
Discussion started: 20 November 2018

Atmospheric Chemistry and Physics Discussions

where f_{xx} is the flux of CO_2 from reservoir xx to the atmosphere, α_{ff} is the average oxidative ratio of fossil fuels and α_B is the average oxidative ratio of terrestrial organic matter. Knowing f_{ff} and α_{ff} from industrial inventories, and measuring the changes in O_2 and CO_2, we can solve these two equations for f_{land} and f_{ocean} in terms of α_B (for a rigorous treatment of these equations, see for example Battle et al. (2000)). This O_2-based method has become increasingly sophisticated with refinements in methodology, and increasingly precise with better instruments and ever-longer datasets (Keeling and Manning, 2014). Nonetheless, all estimates of carbon fluxes based on atmospheric O_2 require a value for α_B.

The molar ratio of O_2 released to the atmosphere and CO_2 removed from it during photosynthesis (effectively α_B) will depend on the type of organic material being synthesized. This ratio is set by the relative amounts of carbon and hydrogen in the material, as well as the amount and source of any nitrogen included. Similarly, the ratio of CO_2 release and O_2 uptake during respiration depends on the composition of the material being respired. For example, synthesis and respiration of the simplest sugar (glucose: $C_6H_{12}O_6$) will have a flux ratio of 1.0. However, if plants are making shoots and other nitrogen-rich tissue, the oxidative ratio might range from 1.0 to 1.26, depending on the source of the nitrogen (nitrate vs. ammonium) (Bloom et al., 1989). Clearly, any value of α_B that is used in a large-scale calculation of carbon fluxes must represent an average of many processes in many ecosytems for long times.

One approach to this problem is to survey the elemental ratios of various biogenic materials. This was done by Severinghaus (1995); Randerson et al. (2006); Masiello et al. (2008); Hockaday et al. (2009); Worrall et al. (2013) and Gallagher et al. (2017). Based on a variety of techniques and a range of materials, estimates at present seem to be around 1.05 ± 0.1(Keeling and Manning, 2014). Propagating this uncertainty to the global land-ocean partition of carbon uptake corresponds yields a value of ± 0.1pg of carbon/year.

An alternative approach, and the one we have chosen, was first published by Seibt et al. (2004); Sturm et al. (2005) and Stephens et al. (2007). It uses direct measurements of O_2 and CO_2 changes in ambient air within, and close to, an ecosystem. Given sufficient precision and temporal resolution, the covariation of these two atmospheric components should correspond to a whole-ecosystem average value of α_B. The most groundbreaking feature of the work of Stephens et al. (2007) was the use of a newly-developed, continuous O_2 analyzer deployed at the study site, allowing precise, high-frequency measurements. These techniques have the potential to better characterize α_B as well as improve our understanding of the underlying physiology of the ecosytem generating the fluxes.

Following Stephens et al. (2007), we have used a fuel-cell-based differential O_2 analyzer and a non-dispersive infrared (NDIR) CO_2 analyzer to make quasi-continuous measurements of the air in and above the canopy at the Harvard Forest Environmental Measurement Site (Urbanski et al., 2007). In following sections of this manuscript, we begin with a description of the instrument and our methods of data collection and analysis. We then present data acquired between 2006 and 2013 and make a first effort at interpreting these data in the context of both the land-ocean partition and the response of the ecosystem to environmental controls.

Atmos. Chem. Phys. Discuss., https://doi.org/10.5194/acp-2018-1041
Manuscript under review for journal Atmos. Chem. Phys.
Discussion started: 20 November 2018

Atmospheric Chemistry and Physics Discussions

2 Methods

In August 2005 we installed a measurement system at the Harvard Forest Environmental Measurement Site (EMS). Located at 42.537755°N, 72.171478°W and 340m above sea level, we collected air from two intake tubes mounted on a tower 7.50m and 29.0m above the ground. The lower intake is within the forest canopy, the upper about 5m above it. The tower and site are described in more detail by Urbanski et al. (2007). Our system is very similar to the one installed at WLEF in Wisconsin and documented very thoroughly by Stephens et al. (2007), so we focus primarily on differences from the WLEF instrument in our description here.

2.1 System design and operation

A schematic of the system is shown in Fig. 1. Unless otherwise mentioned, all wetted surfaces are stainless steel. At both points of collection, air is drawn in through downward-facing aspirated inlets (R.M. Young, Part #43408) to reduce thermal fractionation (Blaine et al., 2006). A nominal flow rate of $50 cm^3 min^{-1}$ is maintained at all times in both lines using pumps with viton diaphragms and PTFE valves (KNF Neuberger N05-ATI) in concert with mass flow controllers (MKS M100B). Tubing on the tower ($\frac{3}{8}'' O.D.$ Dekabon®) is routed into the instrument enclosure without local low spots to minimize buildup of condensed water. Within the building, water is removed from the airstream using a series of three coaxial stainless steel traps. The first is kept at $5°C$ with a Peltier cooler (M&C model ECP2000-SS), while the second and third traps are filled with borosilicate glass beads and immersed in a heat-transfer fluid (Syltherm-XLT®) held at $-90°C$ using a mechanical refrigeration system (FTS VT490). Filters with a nominal pore size of $7\mu m$ (Swagelok SS-6F-7) collect particulates and ice crystals entrained in the airstream exiting the traps. Since our analyzers can only measure a single airstream, the high and low intake lines are alternately sent to analysis or waste, with the selection switched every 720 seconds by a pneumatically actuated, crossover ball valve with PTFE packing (Swagelok SS-43YFS2).

Both the O_2 and CO_2 analyzers make differential measurements of the chosen stream of ambient air relative to a cylinder of dried air (the working tank, WT). Data are recorded at $1Hz$. Periodically, the ambient air stream is diverted to waste and the WT is analyzed against one of four calibration tanks: HS, LS, MF and LF. Details of the various tanks are given in Table 1. The frequency of the calibration runs was determined in part from pre-deployment tests in which we observed instrumental drift when running pairs of (sacrificial) tanks against one another. Other considerations include consumption of standard gases and lost time for atmospheric measurements.

The ambient air stream (high or low) or the calibration tank is chosen for analysis with a pair of electrically actuated 6-port selector valves (VICI EMT2SF6MWE and EMT2SDMWE). From these valves it passes through another mass flow controller, the NDIR CO_2 analyzer (Licor LI-7000), a $0.5\mu m$ filter (Swagelok SS-6F-05), a needle-tipped metering valve (Swagelok SS-4BMG), a changeover valve assembly (four Numatics TM101V24C2 solenoid valves on a custom-built aluminum manifold), the fuel-cell based O_2 analyzer (Sable Systems Oxzilla II with customized stainless steel internal plumbing) and exits through a mass-flow meter (Honeywell AWM3100V). Absolute pressures are recorded upstream of the CO_2 analyzer in three locations (Omega PX303-030A10V) and within the Oxzilla (see below).

Atmos. Chem. Phys. Discuss., https://doi.org/10.5194/acp-2018-1041
Manuscript under review for journal Atmos. Chem. Phys.
Discussion started: 20 November 2018

Atmospheric Chemistry and Physics Discussions

The response of the Licor CO_2 analyzer depends on the pressure difference between the two cells. Thus, we use a differential manometer and electronically controlled metering valve with active feedback (MKS 223BD, 247D and 248) to ensure balanced pressures in the Licor.

The response of the Oxzilla O_2 analyzer depends on both pressure and flow differences between the cells. To provide sufficient control of these parameters, we have two metering valves upstream of the Oxzilla and one downstream. We use the metering valves (as well as the active pressure-difference control upstream of the Licor) to tune the system so that pressures and flows are as close to equal as possible regardless of the state of the changeover valve (see below). For this tuning, and subsequent monitoring of the system, we use flow data from the Honeywell meters and pressure data recorded within the Oxzilla immediately downstream of the cells. Prior to deployment, we modified the Oxzilla's internal plumbing and electronics so that pressure transducers (Honeywell SCX15N) were teed off of each of the outlets of the fuel cells. The two transducers are read out with the single high-precision digitizer built into the Oxzilla motherboard using a multiplexer to alternately select the transducer signal sent to the digitizer.

To further improve measurement precision of O_2, we follow Stephens et al. (2007) and use a changeover valve to alternate the fuel cells into which the two gas streams flow. This allows for a difference-of-difference calculation that eliminates cell-to-cell biases in the instrument. However, the elimination of bias occurs only if that bias varies little during the two measurement periods being considered. Achieving optimal precision would seem to require high frequency changeovers to reduce variation in the bias. However, each changeover is followed by a "dead time" when flows and instrument response need to settle. For a given dead time, more rapid changeovers means fewer measurements are available for averaging, leading to a greater impact of random noise and thus, poorer precision.

We adopt a method for quantifying this trade-off and settling on an optimal changeover frequency that was developed by Keeling et al. (2004). We determined dead time for our instrument by analyzing tank air (relative to a working tank) with the changeover running very slowly. We then measured the time after each changeover required for O_2 values to settle to within 1σ of the post-changeover equilibrium value. This "dead time" was 14 seconds for our instrument. We then determined the optimal changeover time by analyzing two tanks of air against each other with the changeover valve disabled. We processed these measurements as if the changeover valve were operating, calculating difference-of-difference values for various (hypothetical) changeover rates, imposing a $14s$ dead time. This exercise indicated an optimal changeover rate of $24s$ between switches.

2.2 Data reduction

2.2.1 Atmospheric data

In order to allow the instrument to achieve equilibrium after the selector valves have changed state (at the end of a calibration run), we discard the first $432s$ of atmospheric data after such an actuation.

The remaining atmospheric data are naturally divided into 12-minute subsets by the switching of the intake selector between high and low intake lines. We discard the first $432s$ of data after an intake switch to allow time for the instrument to reëquilibrate after the disruption in flows and pressures. The surviving data are processed slightly differently for O_2 and CO_2.

Atmos. Chem. Phys. Discuss., https://doi.org/10.5194/acp-2018-1041
Manuscript under review for journal Atmos. Chem. Phys.
Discussion started: 20 November 2018

Atmospheric Chemistry and Physics Discussions

For O_2, we break the surviving $288s$ of data into $24s$ blocks defined by the cycling of the changeover valve. We average the $1Hz$ data collected between $14s$ and $24s$ after the valve changes state. We then calculate difference-of-difference values for consecutive pairs of averages. This typically yields 6 values. These are in turn averaged, yielding a single O_2 value for the chosen intake height at a time corresponding to the middle of the interval of data used in the average.

For CO_2, we consider every $1Hz$ CO_2 value collected at the same time as the $1Hz$ O_2 values that contribute to the final O_2 mixing ratio for each of the 12-minute intake intervals. After the cuts for deadtime following valve actuations (gas selector, intake selector and changeover), there are 120 of live data. Thus, we average the 120 "live" values for a single CO_2 mixing ratio with the same time-stamp as the O_2 value.

2.2.2 Calibration data

Roughly four times daily, atmospheric sampling is interrupted for 6-minute runs of calibration tanks. To more effectively use the information from these runs, we adopt a protocol that differs from our treatment of atmospheric data.

To purge stale gas from the lines, air from the calibration tank is vented to waste for 6 minutes prior to measurement. Once the selector valves direct the calibration air to the analyzers, we consider all 6 minutes of CO_2 measurements. We look for a transition in the CO_2 value as tank air reaches the analyzer, displacing the atmospheric air that was in the atmosphere. We find the time at which 70% of the eventual change in CO_2 has been achieved and consider all subsequent data.

To determine O_2 in these calibration runs, we calculate difference-of-differences values for each pair of changeover blocks as with our atmospheric data. Then, based on the timing of the transition in the CO_2 record, we average the last 3, 4, or 5 difference-of-difference values of the calibration run.

To determine CO_2, we average all CO_2 values collected at the same times as the values that were used in the O_2 calculation.

Our standards are calibrated on the Scripps S2 O_2 scale (Keeling et al., 1998, 2007) and the NOAA/WMO CO_2 scale(Zhao and Tans, 2006), thanks to the generous assistance of these laboratories. Thus it is on these scales that we report our measurements.

2.3 System performance

To determine the instrumental precision, we use runs of calibration tanks (see Sec. 2.2.2). σ_{O_2} is derived from the scatter in the 3, 4, or 5 difference-of-difference values about their mean. Similary, σ_{CO_2} is derived from the scatter of the 30, 40, or 50 individual CO_2 values used when calculating the CO_2 mixing ratio for each standard tank. We refer to this metric as "scatter on one tank" (SOOT).

Results of these calculations are shown in Fig. 2. Not surprisingly, the performance of the instrument varies over time. At some times a degradation in precision can be traced to problems with an individual instrument, while at other times water (liquid or solid) in the system was found to be the cause. The major fall-off in precision that develops in late 2012 and persists until the end of our dataset is most probably due to a leak in the intake selector valve. After removing the instrument for an overhaul, we found the packing nut on the valve had worked loose, leading to leaks.

Atmos. Chem. Phys. Discuss., https://doi.org/10.5194/acp-2018-1041
Manuscript under review for journal Atmos. Chem. Phys.
Discussion started: 20 November 2018

Atmospheric Chemistry and Physics Discussions

We defer a more detailed discussion of instrument performance for a later publication, but based on Fig. 2, we assume $\sigma_{O_2} = 2.0$ and $7.6 \mu mol\ mol^{-1}$ and $\sigma_{CO_2} = 0.2$ and $1.0 \mu mol\ mol^{-1}$ for the precision of individual O_2 and CO_2 values before and after 2012, respectively.

For atmospheric measurements, the O_2 value for a 12-minute run on either the high or low intake is calculated from 6 difference-of-differences pairs, and the CO_2 value is an average of 120 individual measurements (Sec. 2.2.1). Thus, when calculating the covariation of O_2 vs. CO_2, we use $\sigma_{O_2} / \sqrt{6}$ and $\sigma_{CO_2} / \sqrt{120}$ respectively in our Deming regressions.

While we have made great efforts to calibrate our measurements to internationally accepted CO_2 and O_2 scales using our suite of reference tanks (Table 1), we defer a detailed treatment of long-term measurement stability and accuracy for a later publication. Our focus in this manuscript is on α_B, as expressed in a series of short-term averages of CO_2 and O_2 covariation. Thus, our primary concern is instrumental precision and stability over periods of roughly 6 hours.

As a test of our estimates of σ_{O_2} and σ_{CO_2} (above), we can look at the scatter in the 6-minute measurements of our standard tanks. These measurements are typically averages of 4 O_2 values and 80 CO_2 values, leading to expected uncertainties of 0.5 and 0.02 $\mu mol\ mol^{-1}$ respectively. However, the scatter in pre-2012 calibration runs spaced 6 hours apart show single-measurement uncertainties of 1.6 and $0.12 \mu mol\ mol^{-1}$ for O_2 and CO_2 respectively.

These values are substantially larger than expected from the SOOT calculation above. The degraded precision is most likely associated with the changing of our gas-stream selection valve, since this is not captured in our SOOT value. While this will be an added challenge when establishing a long-term calibration record, it has little impact on our measurements of α_B because the gas-stream selection valve is largely inactive during the 6-hr periods over which slopes are calculated.

3 Observations

The measurements we present here commenced on September 27, 2006 and continued until January 9, 2013. The record is approximately continuous until the middle of 2010, when a series of hardware failures, due in part to a lightning strike, caused an extended hiatus in data collection. Measurements resumed in May of 2012 and continued without interruption through the end of that year, when failure of the oxygen analyzer led to a suspension of data collection.

Measurements of O_2 and CO_2 for the entire period of record are shown in Fig. 3, while Fig. 4 gives an example of a single day's cycle. The values shown here were derived from the raw data using the calibration runs and the algorithm described in Sec. 2.2. They represent our best estimates of the O_2 and CO_2 content of the atmosphere on the Scripps S2 and NOAA/WMO scales, respectively. In these figures we can see a very gradual rise in CO_2 and drop in O_2 (due to fossil fuel combustion), a strong diurnal cycle with inverse variation in CO_2 and O_2, and a great deal of variability on a range of time scales. Results from the upper and lower intakes are quite similar, but not identical.

While these records contain a wealth of information, our particular focus is on the covariation of O_2 and CO_2. We expect to see different results from the high and low intakes, particularly at night. The lower intake is more likely to show soil and canopy fluxes, particularly at night when the atmosphere is more stable and the surface layer is more likely to be decoupled

Atmos. Chem. Phys. Discuss., https://doi.org/10.5194/acp-2018-1041
Manuscript under review for journal Atmos. Chem. Phys.
Discussion started: 20 November 2018

Atmospheric Chemistry and Physics Discussions

from the planetary boundary layer. For this reason, we separate the data from the high and low intakes, create day and night subsets for each intake, plot O_2 vs. CO_2 for each subset, perform a linear regression, and take α_B from the slope of the fit.

The 6-hour subsets making up each plot are 9am - 3pm (day) and 10pm - 4am (night). These intervals are chosen to be times of maximal and minimal coupling (day and night, respectively) between the air within and above the canopy. We define the intervals based on the climatological diurnal cycle in the friction velocity $u^\star$ measured at the EMS tower (Munger and Wofsy, 2017). Subsets with fewer than three measurements are ignored. Because uncertainties in both species are comparable, we use a Deming regression (Deming, 2011). Furthermore, to reduce any influence of non-Gaussian tails in the dataset, we perform an iterative fit, in which we calculate the standard deviation of the residuals to the fit (σ_{res}) and discard any points lying more than $4\sigma_{res}$ from the fit. Of the 3760 fits, only 50 had any outliers and only 11 of these required more than one iteration to converge. Representative plots and fits are shown in Fig. 5.

In total, we have slope values for 3760 6-hr subsets. While the great majority of slope values are close to -1.0 and are normally distributed (see Fig. 6), a small number are implausibly large (up to $+2035.9$) or small (down to -102.6). Since we seek a representative slope value for each high/low day/night subset, we choose to limit the impact of these outliers by performing an iterative calcuation of the means. We calculate a mean and standard deviation, discard all slopes more than 3σ from the mean and iterate to convergence. Table 2 shows the results of these calculations, as well as sensitivity studies varying the length of the day and night intervals and the tightness of the cut in our iterative averaging.

4 The basis for interpreting the slope of O_2 vs. CO_2 as α_B

In its simplest form, the variability in O_2 and CO_2 in the continental interior is a two-end-member mixing problem: Fossil fuel fluxes will give slopes around 1.4 (Keeling and Manning, 2014), biogenic fluxes will give slopes close to 1.1 (or lower), and air masses exposed to both types of fluxes will evolve with an intermediate slope. While there are some complications to this simple picture (discussed below), this conceptual framework generally holds.

Within this framework, a successful effort to extract α_B from the data depends on the relative sizes of the biogenic and anthropogenic fluxes. Only at times when photosynthesis and respiration dominate the land-air fluxes will observed slopes be close to α_B.

To justify these assertions, we first use a simple 1-dimensional box model to establish the validity of the end-member mixing framework. We then use a Lagrangian transport model to estimate the region over which surface fluxes influence signals at our sampling site. Finally, estimate the relative size of the biogenic and anthropogenic fluxes.

4.1 "Mixing" of slopes

To test the applicability of a 2-end-member approach, we developed a 1-dimensional box model, in which parcels of air travel forward in time in 12-minute steps, passing over a landscape with forested, suburban and urban components. Fluxes of CO_2 and O_2 move from surface to parcel and vice versa, changing the composition of the parcel over the time step according to

$$C_{end} = C_{start} + \frac{F \cdot t}{h} \frac{22.4}{1000} \quad (1)$$

Atmos. Chem. Phys. Discuss., https://doi.org/10.5194/acp-2018-1041
Manuscript under review for journal Atmos. Chem. Phys.
Discussion started: 20 November 2018

Atmospheric Chemistry and Physics Discussions

where C is the mixing ratio of O_2 or CO_2 in $\mu mol\ mol^{-1}$, F is the flux from the landscape underneath the box in $\mu mol\ m^{-2}\ s^{-1}$, t is the time step in seconds, h is the height of the box in m, and the factors of 22.4 (the molar volume) and 1000 convert moles to liters and liters to m^3, respectively. For h we use one half of the PBL height, based on the value used in more sophisticated models of atmospheric transport (Sargent, 2018; Lin et al., 2003). We spin up the model for 24 hours and then record O_2 and CO_2 concentrations of consecutive parcels as they "arrive" in their final time steps over the same 6-hour day and night intervals used for the observations.

The CO_2 surface fluxes vary with time of day and day of year and are based on observations at Harvard Forest (Munger and Wofsy, 2017) and in urban (Bergeron and Strachan, 2011; Velasco and Roth, 2010; Ward et al., 2015) and suburban (Bergeron and Strachan, 2011) settings. The O_2 surface fluxes were derived from the CO_2 fluxes by assuming exchange ratios of 1.4 for fossil fuel combustion and 1.05 for biospheric activity. The PBL values are climatological hourly average values, calculated separately for summer and winter from the NAM12 dataset (NOAA, 2018). We performed sensitivity studies, varying the landscape composition, surface flux magnitude and PBL height. In all cases, the CO_2 and O_2 values of the parcels entering the model were held constant, ensuring that any variability predicted by the model was a purely local signal.

In all but a few special circumstances, the model predicts slopes that are completely consistent with the specified admixture of the source fluxes over which the air parcels have traveled. Exceptions arise when the covariation of the boundary layer height and diurnal cycles in the fluxes conspire to bias slopes by a few percent. Results of various sensitivity tests and a discussion of these exceptions can be found in Conley (2018), along with a more complete description of the model and its forcing fluxes.

4.2 Region of influence

We use a Lagrangian transport model to estimate the surface regions to which air parcels are exposed during the six hours prior to their arrival at the EMS tower. Specifically, we created back trajectories for a range of dates and times, day and night, across seasons and years using the HYSPLIT Lagrangian transport model (NOAA, 2018) forced with NAM12 meteorology. We generated many sets of six 6-hour back trajectories originating hourly during the daytime or nightime intervals to show the region of influence at Harvard Forest. An example of one such set of trajectories is shown in Fig. 7.

In general, the region of influence ranges from 50km to 200km, with little spatial variation over the 6-hour interval. The air arriving at our study site has travelled over a mostly forested landscape, occasionally passing small urban centers. This analysis is consistent with the work of Gerbig et al. (2006) who found a dramatic fall-off in the influence of fluxes more than $\sim$ 100km from the study site.

4.3 The relative size of fluxes

The relative weighting for combustion and biogenic influence will depend on the magnitudes of the respective fluxes across the region. Our best estimate of combustion fluxes comes from Sargent et al. (2018), who use an inverse analysis of CO_2 concentation data in Massachusetts with a high-resolution prior emission inventory developed specifically for the region (Gately and Hutyra, 2017). Their value of $-0.8kg\ m^{-2}\ y^{-1}$ corresponds to $-0.6\mu mol\ m^{-2}\ s^{-1}$ for the region surrounding Harvard Forest.

Atmos. Chem. Phys. Discuss., https://doi.org/10.5194/acp-2018-1041
Manuscript under review for journal Atmos. Chem. Phys.
Discussion started: 20 November 2018

Atmospheric Chemistry and Physics Discussions

For the biogenic fluxes, we use eddy-flux measurements of net ecosystem exchange (NEE) at Harvard Forest (Munger and Wofsy, 2017). In the summer, the daytime mean NEE at Harvard Forest is of order $10-20 \mu mol\ m^{-2}\ s^{-1}$ for coniferous and deciduous forest respectively, and around $5 \mu mol\ m^{-2}\ s^{-1}$ at night. Winter NEE averages range from 2 to 3 $\mu mol\ m^{-2}\ s^{-1}$.

Taken together, these results show the regionally averaged biogenic influence on CO_2 (and by extension O_2) is 10-20 times the combustion influence. The dominance of the biogenic influence is also clear in the modeling results of Gerbig et al. (2006), which show short-term variability in CO_2 is dominated by the predicted influence of vegetation. The influence of fossil fuel is generally small. Continental background defines the mean value, but has very little impact on the diel cycle.

5 Discussion of observations

Based on the arguments presented above, we treat the slopes of our plots as averages of α_B (a number near 1.0) and α_{ff} (~ 1.4) weighted by the relative contributions of these fluxes in the Harvard Forest "footprint".

Taking all data together, using 6-hour intervals and a 3σ iterative cut, if we simply treat the slope as a direct indication of the exchange ratio, we get $\alpha_B = 1.058 \pm 0.006$ (see Tab. 2). This result is in agreement with the values for α_B calculated by Worrall et al. (2013) and at the low end of the range quoted by Severinghaus (1995). It is significantly lower than the value of 1.1 used in most calculations of the land carbon sink (Keeling and Manning, 2014).

Further confirmation of the end-member model comes from considering 2-week aggregation periods (instead of 6 hours). Here we find the slopes average -1.19 ± 0.02. This is consistent with nearly equal contributions from fossil and biotic fluxes, as expected for an aggregation period with an effective footprint encompassing the entire continental United States (Gerbig et al., 2006).

5.1 Day-night comparisons

Considering subsets of the data (Tab. 2) may provide insight into the processes determining observed slope values. For example, the night slopes are steeper than day slopes at each intake height.

One possible explanation for steeper nighttime slopes is a fossil fuel contribution whose significance is enhanced by trapping in the surface layer (Munger, 1996). Fossil fuel influence may be more apparent at night when biotic fluxes change sign and are reduced (Munger and Wofsy, 2017) but fossil fuel combustion falls only slightly (Bergeron and Strachan, 2011; Velasco and Roth, 2010; Ward et al., 2015). During summer days in particular, the biotic and fossil fuel fluxes are opposed, while at night they work together. This explanation is complicated by the growth of the mixed layer in the first half of the day, as near-surface air bearing the signature of nighttime respiration (high CO_2 and low O_2) mixes with air from aloft.

Alternatively, α_B itself might change if, for example, plant respiration shifts to molecules richer in nitrogen with higher oxidative ratios (*i.e.* steeper slopes) (Keeling and Manning, 2014). The problem with this explanation is that the respired material must have been synthesized prior. In other words, in the long term, fluxes must balance and we should see daytime periods with similarly steep slopes. Given that our data come from all seasons over multiple years, such a persistent imbalance seems unlikely.

Atmos. Chem. Phys. Discuss., https://doi.org/10.5194/acp-2018-1041
Manuscript under review for journal Atmos. Chem. Phys.
Discussion started: 20 November 2018

Atmospheric Chemistry and Physics Discussions

It is also clear from eddy flux data at Harvard Forest that soil respiration has a strong influence at night, particularly at the low intake (Urbanski et al., 2007). If the respired soil organic matter has a larger-than-average α_B, it would explain our observed day/night difference.

While this soil organic matter must have been synthesized in the recent past, the potential for a greater temporal lag between on-the-tree synthesis and in-the-soil respiration allows the possibility of a biosphere not entirely in balance during our measurement period. Although we can't rule out this explanation, istopic measurements by Wehr and Saleska (2015) imply a residence time for respired carbon of a week or less; evidence that our day-night difference in slopes is unlikely to be due to different oxidative ratios in the synthesized and respired organic materials.

5.2 High-low comparisons

Focusing instead on differences associated with height, we see the high-intake data show steeper slopes than the low-intake data (1.11 vs 1.04 and 1.06 vs 0.97, night and day respectively).

The difference between high and low intakes may result from the atmospheric dynamics within and below the canopy surface layer. Reduced air velocities within the canopy may enhance local influence and drive slope values towards α_B. At night, stratification may increase the isolation of the high intake from the low intake. The high intake senses a large region with variations reflecting regional influences. The low intake is more strongly influenced by the immediate surroundings. Said differently, a high/low split in the dataset might better described as a regional/local split.

During the day, the slope for the low intake is particularly shallow—at the low end of values for α_B calculated by Worrall et al. (2013). In contrast to the atmospheric boundary layer, which becomes stable at night, air within the forest canopy can be more stable during the day. This arises because air is warmed from above by incoming sunlight striking leaves, creating a temperature inversion (Jacobs et al., 1992). While this stability might explain the shallow day-low slopes, profiles of CO_2 and O_2 on the tower show that at Harvard Forest these inversions are often eroded by gusts from above penetrating the canopy and usually only persist in the first meter or two above ground level. Thus, this possible mechanism for very shallow slopes in the day-low data seems unlikely and an firm explanation remains elusive.

5.3 Temporal variability in slopes

Our data are sufficiently abundant that we can examine the values of slopes as a function of time. Spectral analysis (using Lomb-Scargle periodograms to accommodate our irregularly spaced data (Press et al., 2007)) shows very few significant peaks (Fig. 9). There is some evidence of a seasonal cycle (1 cycle/year) in the all-inclusive dataset (not shown), which appears to be mostly due to the night-high subset. There is also a suggestion of multi-year variation (0.6 cycles/year) in the day-low dataset and 3-week cycles ($f = 18$) in the day-high and night-low data.

Identical analyses of environmental variables measured at Harvard Forest (temperature, net ecosystem exchange, ecosystem respiration, photosynthetically active radiation and $u^\star$) all show highly significant seasonal and daily cycles, as expected.

The seasonal cycle in slopes may be due to seasonal changes in α_B itself. Trees synthesize many different compounds throughout the year (Seibt et al., 2004), each with their own oxidative ratios (Bloom et al., 1989). However, direct measure-

Atmos. Chem. Phys. Discuss., https://doi.org/10.5194/acp-2018-1041
Manuscript under review for journal Atmos. Chem. Phys.
Discussion started: 20 November 2018

ments of leaves and tree-rings indicate oxidative ratios in these tissues appear invariant through the year (Gallagher et al., 2017).

On the other hand, the total amount of biological activity unquestionably varies seasonally, while the fossil fuel contribution remains roughly constant. Earlier work at Harvard Forest using carbon monoxide and acetylene (Potosnak et al., 1999) shows clearly that fossil fuel combustion is a strong driver of CO_2 variability in the winter, but is overwhelmed by biotic signals during the summer. Thus, the simple seasonal shift in the biotic/fossil-fuel balance is a likely explanation for some, if not all, of the seasonal cycle in slopes.

The three-week cycle in the day-high and night-low records is perplexing. No such cycle appears in the environmental variables listed above. Thus, our working hypothesis is that the 3-week cycles is an experimental artifact resulting from the timing of runs of calibration tanks and swapping of working tanks.

5.4 Selecting periods of heightened biogenic signal

Given the competition between biogenic and anthropogenic in our observations, we searched for periods when the biogenic contribution might be most dominant. This involved selecting for times when the fluxes in the immediate neighborhood were likely to dominate. Our assumption is that background variation is likely to carry signals of continental-scale gradients with more substantial fossil fuel influences embeded therein.

One approach we considered was based on $u^\star$. We hypothesized that slopes calculated when $u^\star$ was low were more likely to be biogenic, since the air at our intakes was exchanging minimally with the overlying boundary layer. However, a scatter plot of slopes as a function of $u^\star$ showed no correlation. Similarly, slope values were insensitive to discrete cuts on average $u^\star$ ($< 40cm\ s^{-1}$), maximum $u^\star$ ($< 50cm\ s^{-1}$) and the scatter in $u^\star$ ($\sigma_{u^\star} < 10cm\ s^{-1}$).

We also explored the possibility of a link between slopes and the ranges of CO_2 and O_2 during the 6-hour periods. Again, no correlation was apparent, whether with discrete cuts during summer and winter periods separately, or with scatter plots of slope vs. range.

We tested the hypothesis that summer periods of extended high barometric pressure with languid anticyclonic circulation might be dominated by local fluxes. Again, we observed no correlation between slope and barometric pressure, whether with discrete cuts or with scatter plots.

Finally, we looked for correlations between slopes and wind speed, direction and variability. We found none, even when winds were from the relatively polluted sector to the southwest.

In short, relatively simple indicators of reduced advective transport show no correlation with shallower slopes. Taken together, the insentivity of our result adds support for our model of a geographically modest footprint comprised of a landscape in which biogenic fluxes are much stronger than anthropogenic ones.

Atmos. Chem. Phys. Discuss., https://doi.org/10.5194/acp-2018-1041
Manuscript under review for journal Atmos. Chem. Phys.
Discussion started: 20 November 2018

Atmospheric Chemistry and Physics Discussions

6 Conclusions

Having measured changes in atmospheric CO_2 and O_2 with a precision of a few $\mu mol\ mol^{-1}$ in a mixed deciduous, mid-latitude forest, we find that these species covary with a molar ratio of 1.058 ± 0.006 (O_2 : CO_2). If our measurements reflect mainly local influences and are representative of a predominantly forested landscape, they support the use of a lower value of α_B than the 1.1 that has been used in recent oxygen-based calculations of global carbon budgets (Keeling and Manning, 2014).

If instead, our data represent a mix of forest and fossil fuel fluxes, 1.058 ± 0.006 is an upper limit on α_B. Adopting a two-end-member mixing model, the best value for α_B would be taken from the subset of the data with the smallest fossil fuel contribution and presumably, the shallowest measured slope. Restricting our dataset to daytime values from the low intake in summer (when we expect local influences to be maximal due to vigorous biotic activity and modest coupling with the air above the canopy), we find $\alpha_B = 1.01 \pm 0.01$.

Further constraining α_B for Harvard Forest will require analyses of the local atmospheric dynamics that are beyond the scope of this work. The validity of applying a single α_B from Harvard Forest in global carbon budgets is also open to question. However, the consistency of elemental ratios in the work of Worrall et al. (2013) across a range of study sites suggests the Harvard Forest result may have broad applicability. Furthermore, basic constraints in plant physiology argue against wildly divergent α_B values across species (Björkman and Demmig, 1987). Nonetheless, studies like this one at other sites are required to ensure the robustness of O_2-based carbon budgets.

If our results are in fact globally applicable, the use of 1.01 for α_B leads to a 9% increase in carbon uptake attributed to the land biosphere and an equivalent reduction in oceanic carbon storage (see Eq. 8 of Keeling and Manning (2014)). While this adjustment is within the uncertainties on these terms in the global carbon budget, it would nonetheless be an important correction.

Data availability. Battle M, Munger W. 2018. Atmospheric Oxygen and Carbon Dioxide at Harvard Forest EMS Tower since 2006. Harvard Forest Data Archive: HF306.

Author contributions. MB conceived of the experiment. MB built and operated the hardware and wrote software with assistance from JWM, ES, RP, RH, ZD, JS, JW, KG, SS and JC. MB and MC performed data analysis. MB wrote the manuscript with assistance JWM and MC.

Competing interests. The authors have no competing interests to declare.

Atmos. Chem. Phys. Discuss., https://doi.org/10.5194/acp-2018-1041
Manuscript under review for journal Atmos. Chem. Phys.
Discussion started: 20 November 2018

Acknowledgements. Analysis of our data was greatly aided by a suggestion from Alessandro Cescatti. We also thank Maryann Sargent for helpful conversations and Taylor Jones for sharing code. Robert Stevens helped with machining, Dj Merrill provided computing support and Emery Boose and John Budney gave invaluable assistance at Harvard Forest.

Operation of the Harvard Forest flux tower site is supported by the AmeriFlux Management Project with funding by the U.S. Department of Energy's Office of Science under Contract No. DE-AC02-05CH11231, and additionally as a part of the Harvard Forest LTER site supported by the National Science Foundation (DEB-1237491). Support for the tower operation during period examined here, as well as partial support for the O_2- CO_2 sampling equipment, came from the U. S. Dept of Energy office of Science through programs that are no longer active (including the National Institute of Global Environmental Change and the National Institute for Climate Change Research). Further support for the sampling equipment was provided by Bowdoin College.

Atmos. Chem. Phys. Discuss., https://doi.org/10.5194/acp-2018-1041
Manuscript under review for journal Atmos. Chem. Phys.
Discussion started: 20 November 2018

References

Battle, M., Bender, M. L., Tans, P., White, J., Ellis, J., Conway, T., and Francey, R.: Global Carbon Sinks and Their Variability Inferred from Atmospheric O_2 and $\delta^{13}C$, Science, 287, 2467–2470, 2000.

Bergeron, O. and Strachan, I. B.: CO_2 sources and sinks in urban and suburban areas of a northern mid-latitude city, Atmospheric Environment, 45, 1564–1573, 2011.

Björkman, O. and Demmig, B.: Photon yield of O_2 evolution and chlorophyll flourescence characteristics at 77K among vascular plants of diverse origins, Planta, 170, 489–504, https://doi.org/10.1007/BF00402983, 1987.

Blaine, T., Keeling, R., and Paplawsky, W.: An improved inlet for precisely measuring the atmospheric Ar/N2 ratio, Atmospheric Chemistry and Physics, 6, 1181–1184, 2006.

Bloom, A., Caldwell, R., Finazzo, J., Warner, R., and Weissbart, J.: Oxygen and carbon dioxide fluxes from barley shoots depend on nitrate assimilation, Plant Physiology, 91, 352–356, 1989.

Conley, M. M.: Using atmopsheric O_2 and CO_2 to determine the stoichiometry of photosynthesis and respiration in a temperate forest, Bachelor of Arts thesis, Bowdoin College, https://digitalcommons.bowdoin.edu/honorsprojects/87/, 2018.

Deming, W. E.: Statistical adjustment of data, Dover Publications, New York, 2011.

Gallagher, M. E., Liljestrand, F. L., Hockaday, W. C., and Masiello, C. A.: Plant species, not climate, controls aboveground biomass O_2:CO_2 exchange ratios in deciduous and coniferous ecosystems, Journal of Geophysical Research: Biogeosciences, 122, 2017JG003 847, 2017.

Gately, C. K. and Hutyra, L. R.: Large Uncertainties in Urban-Scale Carbon Emissions, Journal of Geophysical Research, Atmopsheres, 122, 11 242–11 260, 2017.

Gerbig, C., Lin, J. C., Munger, J. W., and Wofsy, S. C.: What can tracer observations in the continental boundary layer tell us about surface-atmosphere fluxes?, Atmospheric Chemistry and Physics, 6, 539–554, 2006.

Hockaday, W., Masiello, C., Randerson, J., Smernik, R., Baldock, J., Chadwick, O., and Harden, J.: Measurement of soil carbon oxidation state and oxidative ratio by 13C nuclear magnetic resonance, Journal of Geophysical Research: Biogeosciences, 114, https://doi.org/10.1029/2008JG000803, 2009.

Jacobs, A. F. G., van Boxel, J. H., and Shaw, R. H.: The dependence of canopy layer turbulence on within-canopy thermal stratification, Agricultural and Forest Meteorology, 58, 247–256, 1992.

Keeling, R. and Manning, A.: Studies of Recent Changes in Atmospheric O_2 Content, in: Treatise on Geochemistry, pp. 385–404, Elsevier Inc., 2 edn., https://doi.org/10.1016/B978-0-08-095975-7.00420-4, 2014.

Keeling, R., Manning, A., McEvoy, E., and Shertz, S.: Methods for measuring changes in atmospheric O_2 concentration and their application in southern hemisphere air, Journal of Geophysical Research, 103, 3381–3397, 1998.

Keeling, R., Paplawsky, W., and Cox, A.: On the long-term stability of reference gases for atmospheric O_2/N_2 and CO_2 measurements, Tellus Series B – Chemical and Physical Meteorology, 59, 3–14, 2007.

Keeling, R. F. and Shertz, S. R.: Seasonal and interannual variations in atmospheric oxygen and implications for the global carbon cycle, Nature, 358, 723–727, 1992.

Keeling, R. F., Blaine, T., Paplawsky, B., Katz, L., Atwood, C., and Brockwell, T.: Measurments of changes in atmospheric Ar/N_2 ratio using a rapid-switching, single-capillary mass spectrometer system, Tellus, 56B, 322–338, 2004.

Lin, J. C., Gerbig, C., Wofsy, S. C., Andrews, A. E., Daube, B. C., Davis, K. J., and Grainger, C. A.: A near-field tool for simulating the upstream influence of atmospheric observations: The Stochastic Time-Inverted Lagrangian Transport (STILT) model, Journal of Geophysical Research: Atmospheres, 108, 4493, 2003.

Masiello, C., Gallagher, M., Randerson, J., Deco, R., and Chadwick, O.: Evaluating two experimental approaches for measuring ecosystem carbon oxidation state and oxidative ratio, Journal of Geophysical Research: Biogeosciences, 113, https://doi.org/10.1029/2007JG000534, 2008.

Munger, J. W.: Atmospheric deposition of reactive nitrogen oxides and ozone in a temperate deciduous forest and a subarctic woodland 1. Measurements and mechanisms, Journal of Geophysical Research Atmospheres, 101, 12 639–12 657, 1996.

Munger, W. and Wofsy, S.: Canopy-Atmosphere Exchange of Carbon, Water and Energy at Harvard Forest EMS Tower since 1991, Harvard Forest Data Archive: HF004, 2017.

NOAA: HYSPLIT - Hybrid Single Particle Lagrangian Integrated Trajectory model, https://ready.arl.noaa.gov/HYSPLIT.php, 2018.

Potosnak, M. J., Wofsy, S. C., Denning, A. S., Conway, T. J., Munger, J. W., and Barnes, D. H.: Influence of biotic exchange and combustion sources on atmospheric CO_2 concentrations in New England from observations at a forest flux tower, Journal of Geophysical Research, 104, 9561–9569, 1999.

Press, W. H., Teukolsky, S. A., Vetterling, W. T., and Flannery, B. P.: 13.8 Spectral Analysis of Unevenly Sampled Data, in: Numerical Recipes: The Art of Scientific Computing, pp. 685–692, Cambridge University Press, Cambridge, third edn., 2007.

Randerson, J., Masiello, C., Still, C., Rahn, T., Poorter, H., and Field, C.: Is carbon within the global terrestrial biosphere becoming more oxidized? Implications for trends in atmopsheric O_2, Global Change Biology, 12, 260–271, https://doi.org/10.1111/j.1365-2486.2006.01099.x, 2006.

Sargent, M.: Personal communication, 2018.

Sargent, M., Barrera, Y., Nehrkorn, T., Hutyra, L., Gately, C., Jones, T., McKain, K., Sweeney, C., Hegarty, J., Hardiman, B., and Wofsy, S.: Anthropogenic and Biogenic CO_2 fluxes in the Boston urban region, Proceedings of the National Academy of Sciences, 115, 7491–7496, 2018.

Seibt, U., Brand, W., Heimann, M., Lloyd, J., Severinghaus, J., and Wingate, L.: Observations of O2: CO2 exchange ratios during ecosystem gas exchange, Global Biogeochemical Cycles, 18, 1–18, https://doi.org/10.1029/2004GB002242, 2004.

Severinghaus, J. P.: Studies of the Terrestrial O_2 and Carbon Cycles in Sand Dune Gases and in Biosphere 2, Ph.D. thesis, Columbia University, 1995.

Stephens, B., Bakwin, P., Tans, P., Teclaw, R., and Baumann, D.: Application of a differential fuel-cell analyzer for measuring atmospheric oxygen variations, Journal of Atmospheric and Oceanic Technology, 24, 82–94, https://doi.org/10.1175/JTECH1959.1, 2007.

Sturm, P., Leuenberger, M., and Schmidt, M.: Atmospheric O_2, CO_2 and $\delta^{13}C$ observations from the remote sites Jungfraujoch, Switzerland, and Puy de Dôme, France, Geophysical Research Letters, 32, 1–4, https://doi.org/10.1029/2005GL023304, 2005.

Urbanski, S. P., Barford, C. C., Wofsy, S. C., Kucharik, C. J., Pyle, E. H., Budney, J., McKain, K., Fitzjarrald, D. R., Czikowsky, M. J., and Munger, J. W.: Factors controlling CO_2 exchange on time scales from hourly to decadal at Harvard Forest, Journal of Geophysical Research-Biogeosciences, 112, 2007.

Velasco, E. and Roth, M.: Cities as net sources of CO_2 : Review of atmospheric CO_2 exchange in urban environments measured by eddy covariance technique, Geography Compass, 4, 1238–1259, 2010.

Ward, H. C., Kotthaus, S., Grimmond, C. S. B., Bjorkegren, A., Wilkinson, M., Morrison, W. T. J., Evans, J. G., Morison, J. I. L., and Iamarino, M.: Effects of urban density on carbon dioxide exchanges: Observations of dense urban, suburban and woodland areas of southern England, Environmental Pollution, 198, 186–200, 2015.

Wehr, R. and Saleska, S.: An improved isotopic method for partitioning net ecosystem-atmosphere CO_2 exchange, Agricultural and Forest Meteorology, 214-215, 515–531, 2015.

Worrall, F., Clay, G. D., Masiello, C. A., and Mynheer, G.: Estimating the oxidative ratio of the global terrestrial biosphere carbon, Biogeochemistry, 115, 23–32, 2013.

Zhao, C. and Tans, P.: Estimating uncertainty of the WMO mole fraction scale for carbon dioxide in air, Journal of Geophysical Research Atmospheres, 111, https://doi.org/10.1029/2005JD006003, 2006.

Atmos. Chem. Phys. Discuss., https://doi.org/10.5194/acp-2018-1041
Manuscript under review for journal Atmos. Chem. Phys.
Discussion started: 20 November 2018

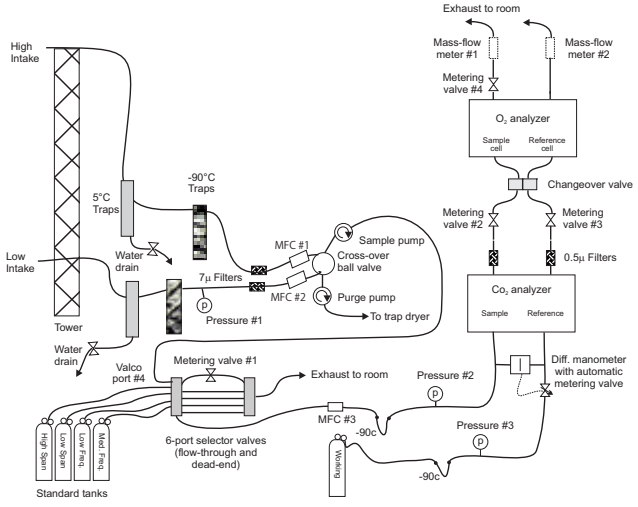

Figure 1. Schematic diagram of the instrumentation installed at Harvard Forest

Atmos. Chem. Phys. Discuss., https://doi.org/10.5194/acp-2018-1041
Manuscript under review for journal Atmos. Chem. Phys.
Discussion started: 20 November 2018

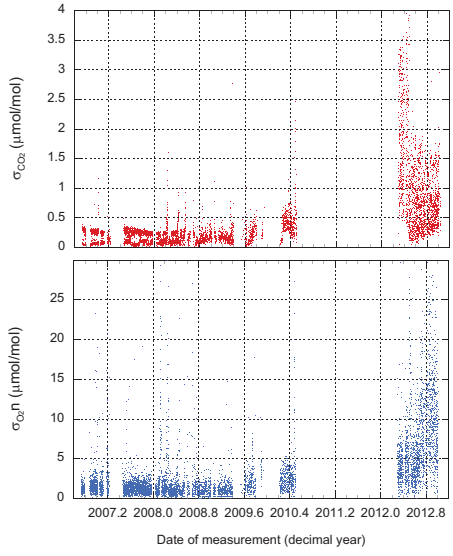

Figure 2. The scatter (standard deviation from the mean) of routine CO_2 and O_2 measurements of calibration tanks. Values plotted here apply to individual CO_2 measurements (1Hz) and single difference-of-difference O_2 values (1/48s).

Atmos. Chem. Phys. Discuss., https://doi.org/10.5194/acp-2018-1041
Manuscript under review for journal Atmos. Chem. Phys.
Discussion started: 20 November 2018

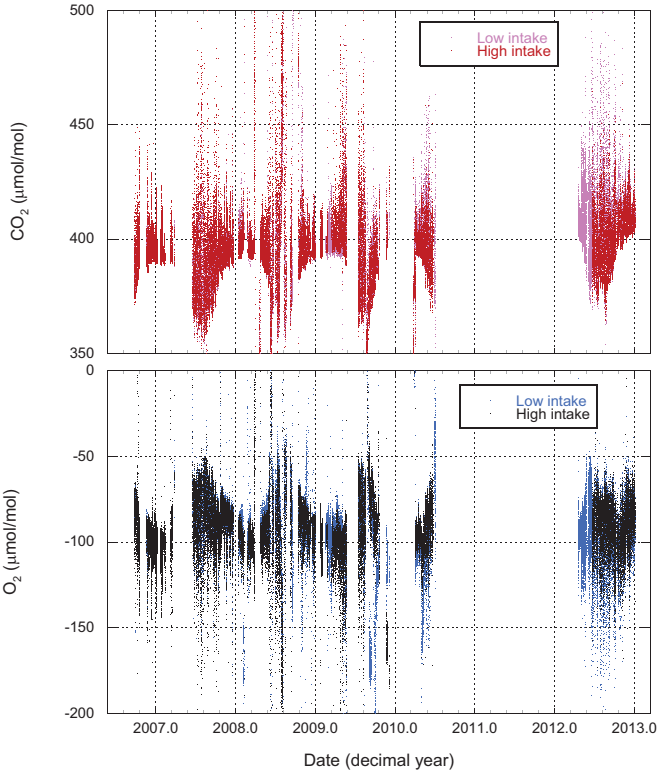

Figure 3. CO_2 and O_2 measured from both high and low intakes at Harvard Forest. The data have been processed (Sec.2.2) and are presented on the WMO and S2 scales. Each point (spaced 11min apart) represents the average atmospheric composition for a $4.8min$ period.

Atmos. Chem. Phys. Discuss., https://doi.org/10.5194/acp-2018-1041
Manuscript under review for journal Atmos. Chem. Phys.
Discussion started: 20 November 2018

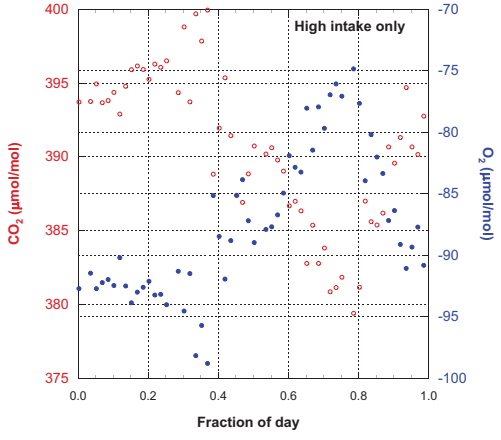

Figure 4. A detail from Fig. 3: CO_2 and O_2 measured from the high intake on Sept. 29, 2006. This is simply one example of the diurnal cycle of these species. Note the strict inverse variation in O_2 and CO_2, even when there are large deviations from a smooth temporal evolution.

Atmos. Chem. Phys. Discuss., https://doi.org/10.5194/acp-2018-1041
Manuscript under review for journal Atmos. Chem. Phys.
Discussion started: 20 November 2018

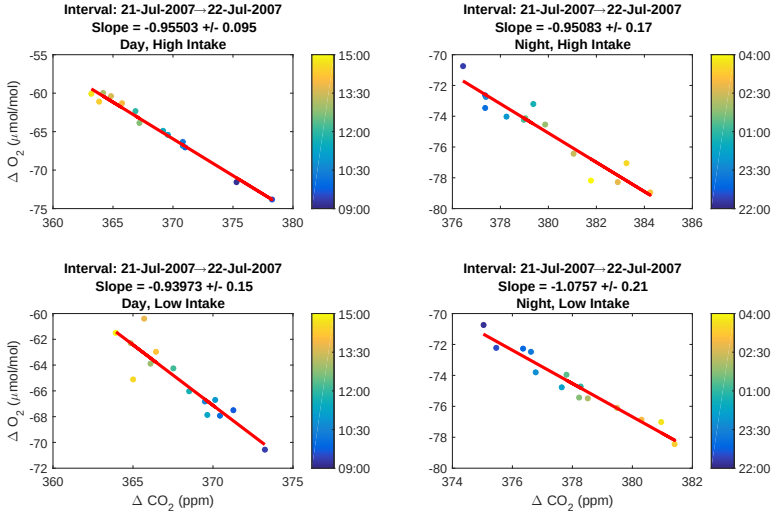

Figure 5. Representative examples of slope-plots: Data collected during day and night periods from the high and low intakes on July 21-22, 2007. The colors of the points indicate the time of collection within the 6-hr intervals, as keyed in the color bar to the right of each plot. Errors on the slopes are purely statistical.

Atmos. Chem. Phys. Discuss., https://doi.org/10.5194/acp-2018-1041
Manuscript under review for journal Atmos. Chem. Phys.
Discussion started: 20 November 2018

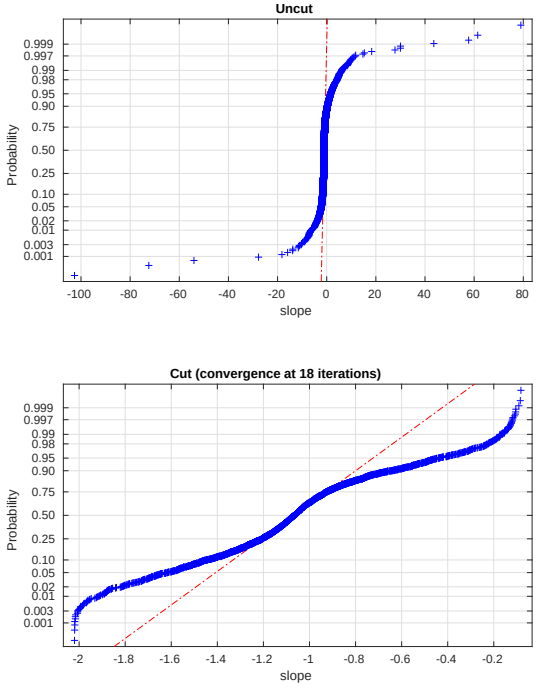

Figure 6. Probability plots of slopes for the entire dataset, before and after a 3σ iterative cut. In the interests of clarity, we omit five points with extremely large or small slopes from the upper panel. See Table 2 for statistical details of these distributions.

Atmos. Chem. Phys. Discuss., https://doi.org/10.5194/acp-2018-1041
Manuscript under review for journal Atmos. Chem. Phys.
Discussion started: 20 November 2018

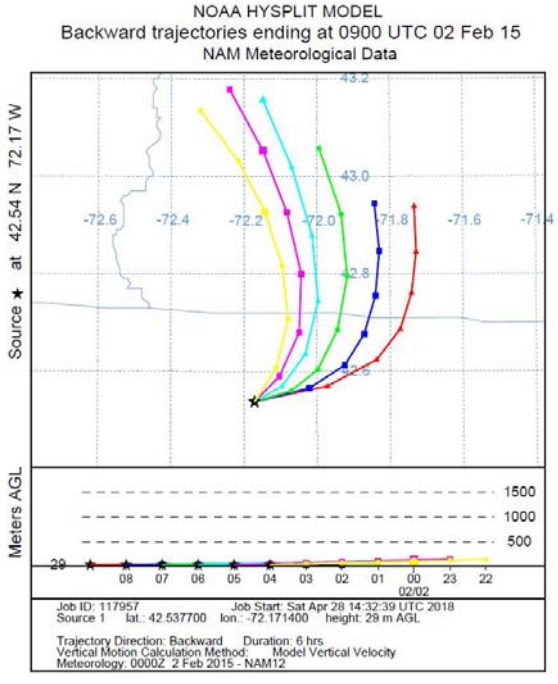

Figure 7. An example of 6-hour back-trajectories for Harvard Forest on Feb 2, 2015. Trajectories start hourly between 10pm and 4am EST, corresponding to the nighttime interval for slope plots. State lines for New Hampshire, Vermont and Massachusetts are in gray. On this particular night, the source region was fairly constant, so changes in O_2 and CO_2 are relatively likely to be primarily due to local influences.

Atmos. Chem. Phys. Discuss., https://doi.org/10.5194/acp-2018-1041
Manuscript under review for journal Atmos. Chem. Phys.
Discussion started: 20 November 2018

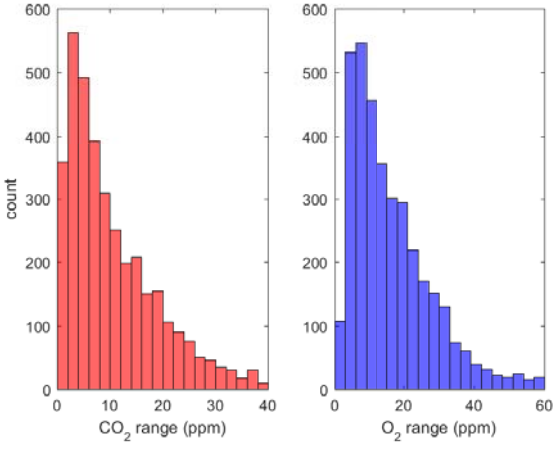

Figure 8. Histograms of the total variation in CO_2 and O_2 for each 6-hour collection period. The upper tails of the histograms were omitted to better show the core of the distributions.

Atmos. Chem. Phys. Discuss., https://doi.org/10.5194/acp-2018-1041
Manuscript under review for journal Atmos. Chem. Phys.
Discussion started: 20 November 2018

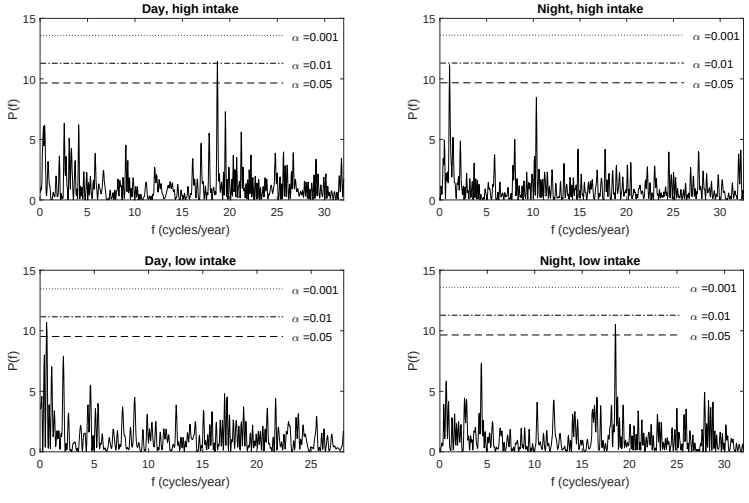

Figure 9. Lomb-Scargle periodograms for the four subsets of the slope values, showing power spectra for a range of frequencies in cycles per year. Dashed lines give the power thresholds for the significance levels labelled.

Atmos. Chem. Phys. Discuss., https://doi.org/10.5194/acp-2018-1041
Manuscript under review for journal Atmos. Chem. Phys.
Discussion started: 20 November 2018

Atmospheric Chemistry and Physics Discussions

Table 1. Nominal composition of calibration tanks. Actual values vary slightly as cylinders are used and refilled.

Tank name	O_2 (per meg on S2 scale)	CO_2 ($\mu mol\ mol^{-1}$)	Analysis frequency
High Span (HS)	+125	350	4/day
Low Span (LS)	-850	525	4/day
Medium Freq. (MF)	-360	375	1/3 days
Low Freq. (LF)	-470	390	1/week

Atmos. Chem. Phys. Discuss., https://doi.org/10.5194/acp-2018-1041
Manuscript under review for journal Atmos. Chem. Phys.
Discussion started: 20 November 2018

Atmospheric Chemistry and Physics Discussions

Table 2. Table of average values for all slopes and the four data subsets. σ is 1 standard deviation, SEM is the standard error on the mean ($\sigma/\sqrt{n}$), and n is the number of slope values surviving the iterative cut. For more details, see Conley (2018).

Interval length and cut	Data set	mean	σ	SEM	n
6-hour (3σ)	All data	-1.058	0.33	0.006	3058
	Day, high intake	-1.06	0.39	0.01	804
	Day, low intake	-0.97	0.36	0.01	703
	Night, high intake	-1.11	0.26	0.01	819
	Night, low intake	-1.04	0.41	0.01	798
4-hour (3σ)	All data	-1.03	0.45	0.01	3009
	Night, high intake	-1.10	0.36	0.01	806
	Night, low intake	-1.08	0.38	0.01	723
	Day, high intake	-0.99	0.54	0.02	781
	Day, low intake	-0.92	0.55	0.02	692
6-hour (4σ)	All data	-0.98	0.60	0.01	3488
	Day, high intake	-0.99	0.76	0.03	904
	Day, low intake	-0.80	0.88	0.03	827
	Night, high intake	-1.08	0.49	0.02	913
	Night, low intake	-0.99	0.59	0.02	851